

## AEGIS: Enhancement of Dust-enshrouded Star Formation in Close Galaxy Pairs and Merging Galaxies up to $z \sim 1$ <sup>1</sup>

Lihwai Lin<sup>2,3</sup>, David C. Koo<sup>3</sup>, Benjamin J. Weiner<sup>4</sup>, Tzihong Chiueh<sup>2</sup>, Alison L. Coil<sup>5,6</sup>,  
Jennifer Lotz<sup>7,8</sup>, Christopher J. Conselice<sup>9</sup>, S. P. Willner<sup>10</sup>, H. A. Smith<sup>10</sup>, Puragra  
Guhathakurta<sup>3</sup>, J.-S. Huang<sup>10</sup>, Emeric Le Floc'h<sup>5</sup>, Kai G. Noeske<sup>3</sup>, Christopher N. A.  
Willmer<sup>5</sup>, Michael C. Cooper<sup>11</sup>, and Andrew C. Phillips<sup>3</sup>

### ABSTRACT

Using data from the DEEP2 Galaxy Redshift Survey and *HST*/ACS imaging in the Extended Groth Strip, we select nearly 100 interacting galaxy systems including kinematic close pairs and morphologically identified merging galaxies. *Spitzer* MIPS 24  $\mu\text{m}$  fluxes of these systems reflect the current dusty star formation activity, and at a fixed stellar mass ( $M_*$ ) the median infrared luminosity ( $L_{IR}$ ) among merging galaxies and close pairs of blue galaxies is twice ( $1.9 \pm 0.4$ ) that of control pairs drawn from isolated blue galaxies. Enhancement declines

---

<sup>1</sup> Some of the data presented herein were obtained at the W. M. Keck Observatory, which is operated as a scientific partnership among the California Institute of Technology, the University of California and the National Aeronautics and Space Administration. The Observatory was made possible by the generous financial support of the W.M. Keck Foundation.

<sup>2</sup>Department of Physics, National Taiwan University, Taipei 106, Taiwan; Email: d90222005@ntu.edu.tw

<sup>3</sup>UCO/Lick Observatory, Department of Astronomy and Astrophysics, University of California, Santa Cruz, CA 95064

<sup>4</sup>Department of Astronomy, University of Maryland, College Park, MD 20742

<sup>5</sup>Steward Observatory, University of Arizona, Tucson, AZ 85721

<sup>6</sup>Hubble Fellow

<sup>7</sup>National Optical Astronomy Observatory, Tucson, AZ 85719

<sup>8</sup>Leo Goldberg Fellow

<sup>9</sup>School of Physics and Astronomy, University of Nottingham, Nottingham NG7 2RD, UK

<sup>10</sup>Harvard-Smithsonian Center for Astrophysics, Cambridge, MA 02138

<sup>11</sup>Department of Astronomy, University of California, Berkeley, CA 94720

with galaxy separation, being strongest in close pairs and mergers and weaker in wide pairs compared to the control sample. At  $\bar{z} \sim 0.9$ ,  $7.1\% \pm 4.3\%$  of massive interacting galaxies ( $M_* > 2 \times 10^{10} M_\odot$ ) are found to be ULIRGs, compared to  $2.6\% \pm 0.7\%$  in the control sample. The large spread of  $L_{IR}/M_*$  among interacting galaxies suggests that this enhancement may depend on the merger stage as well as other as yet unidentified factors (e.g., galaxy structure, mass ratio, orbital characteristics, presence of AGN or bar). The contribution of interacting systems to the total IR luminosity density is moderate ( $\lesssim 36\%$ ).

*Subject headings:* galaxies:interactions - galaxies:evolution - large-scale structure of universe - infrared:galaxies

## 1. INTRODUCTION

Galaxy-galaxy interaction has long been regarded as a key process in galaxy evolution, especially as a mechanism for enhancing star formation during mergers (Larson & Tinsley 1978; Barton et al. 2000). Hydrodynamic  $N$ -body simulations show that active star formation can be triggered by gaseous inflows resulting from mergers of gas-rich galaxies (Mihos & Hernquist 1996; Barnes 2004; Cox 2004). Interaction-triggered star formation is also thought to be responsible for luminous infrared sources. In the local universe, luminous infrared galaxies (LIRGs) and ultra luminous infrared galaxies (ULIRGs) are primarily merging systems (Sanders 1988; Borne et al. 1999). Nevertheless, by studying various star formation indicators of interacting galaxies and normal galaxies, Bergvall, Laurikainen, & Aalto (2003) concluded that galaxy interactions in general are inefficient triggers of starbursts; interactions are a necessary but not sufficient condition to trigger violent starbursts.

The importance of galaxy interactions in the volume-averaged galaxy star formation rate (SFR) remains an open question. Recent studies of mid-IR (MIR) sources at a median redshift of  $z \sim 0.7$  suggest that the IR density at that epoch is dominated by morphologically normal galaxies instead of strongly interacting galaxies (Bell et al. 2005; Melbourne, Koo, & Le Floch 2005). Two main factors may contribute to this result. First, only a small fraction of the galaxy population may be undergoing a major merger at any given time (Carlberg et al. 2000; Bundy et al. 2004; Lin et al. 2004). Second, the overall SFR in normal galaxies at  $z \sim 0.7$  may be enhanced relative to the local population (Bell et al. 2005), perhaps as the result of internal processes such as a higher gas fraction leading to a higher SFR, such that galaxy interactions may have less dramatic effects on triggering star formation at that epoch and/or may be harder to identify. It is the aim of this Letter to examine this second hypothesis.

This Letter presents an analysis of the IR properties of close kinematic galaxy pairs, morphologically selected merging galaxies, and a control sample of randomly selected pairs of isolated galaxies, in the range  $0.1 < z < 1.1$ . In §3 we show our analysis of the IR luminosity ( $L_{IR}$ ) versus stellar mass ( $M_*$ ) for the interacting galaxies and control samples, and the relation between the IR luminosity-to-mass ratio ( $L_{IR}/M_*$ ) and the projected separation of the galaxy pairs. Discussion and conclusions are given in §4. Throughout this Letter we adopt the following cosmology:  $H_0 = 100h \text{ km s}^{-1}\text{Mpc}^{-1}$ ,  $\Omega_m = 0.3$ , and  $\Omega_\Lambda = 0.7$ ;  $h = 0.7$  is adopted when calculating the rest-frame magnitude. Magnitudes are given in the Vega system.

## 2. DATA, SAMPLE SELECTIONS, AND METHODS

### 2.1. Data

The sample used in this Letter consists of  $\sim 4000$  optical selected galaxies with secure redshifts from the DEEP2 Galaxy Redshift Survey and MIPS imaging in the Extended Groth Strip (EGS) region. The EGS has extensive multi-wavelength observations from both the ground and space, coordinated by the All-Wavelength Extended Groth International Survey (AEGIS) team (Davis et al. 2007). The spectral resolution of the DEEP2 survey is  $R \sim 5000$ , corresponding to redshift errors of  $\sim 30 \text{ km s}^{-1}$ , allowing us to define kinematic pairs (see § 2.2). The average sampling rate of the slit placed on galaxies is  $\sim 60\%$ , and the average redshift success is  $\sim 73\%$  (Willmer et al. 2006). Details of the survey and  $K$ -correction procedure are described in a series of DEEP2 papers (Davis et al. 2003; Coil et al. 2004; Willmer et al. 2006). The MIPS (Multiband Imaging Photometer for Spitzer; Rieke et al. 2004)  $24 \mu\text{m}$  observations used here were carried out on 2004 June 19 and 20; Davis et al. (2007) provide further details.

### 2.2. Selection of Kinematic Pairs, Merging Galaxies, and Control Samples

Three classes of galaxy samples are investigated in this study: kinematic pairs, merging galaxies, and a control sample of randomly selected pairs of isolated galaxies, in three redshift bins in the range  $0.1 < z < 1.1$ . To select **kinematic galaxy pairs**, we use the following criteria: (1) For each galaxy in the spectroscopic redshift sample, we first search for any kinematic companions with a relative line-of-sight velocity  $\Delta v \leq 500 \text{ km s}^{-1}$  and a projected physical separation (onto the plane of the sky)  $\Delta r_p < 300 h^{-1}\text{kpc}$ . (2) Among these companions, close pairs are identified such that they satisfy  $\Delta r_p \leq 50 h^{-1}\text{kpc}$  (Patton et al.

2002; Lin et al. 2004). We find a total of 56 close pairs. (3) For comparison, wide pairs are identified as kinematic companions with  $50 h^{-1}\text{kpc} \leq \Delta r_p \leq 300 h^{-1}\text{kpc}$ , and we retain only wide pairs that are closest companions to each other (such that there is only one wide pair companion per galaxy). The spectroscopic redshift sample is not entirely complete, however; it is possible that for a given galaxy, there exists a closer companion that is missing in the redshift sample. Therefore,  $\Delta r_p$  for each paired system is an upper limit on the actual distance to the closest companion. To minimize this effect we also search for photometric companions of each galaxy, and we keep only those wide pairs that do not have a photometric companion (with observed  $\Delta m_R < 1$  mag) within  $\Delta r_p \leq 30 h^{-1}\text{kpc}$ , for a sample of 126 wide pairs. (4) Absolute magnitude limits were applied to all pair samples within a given redshift bin (see Table 1). (5) To study the effect of interactions between two gas-rich galaxies, we further applied a color cut using rest-frame  $U - B = 0.25$  as the division between blue and red galaxies and only include blue galaxies in our samples. It is possible that we have missed some red, dusty, late-type galaxies due to our color selection. However, the number density of that population is  $\sim 8\%$  compared to the blue galaxy population (Weiner et al. 2005) and is therefore negligible for our analysis.

We also define a set of morphologically identified **merging galaxies** using a subsample of blue galaxies in the EGS that have deep *HST* images taken with Advanced Camera for Surveys (ACS) as part of GO program 10134 (PI: M. Davis). These morphologically identified merging galaxies are preferentially in strongly interacting systems and are in a different merger stage than the kinematic close pairs. We identify merging galaxies using three non-parametric parameters: the Gini coefficient ( $G$ ), the second-order moment of the brightest 20% of a galaxy’s pixels ( $M_{20}$ ), and the asymmetry measurement ( $A$ ), all of which have been shown to identify merger candidates (Conselice 2003; Conselice et al. 2003; Lotz, Primack, & Madau 2004). We first select galaxies with morphological parameters of  $G > -0.115 * M_{20} + 0.384$  or  $A > 0.25$  (see Lotz et al. 2007 for discussion on  $G$  and  $M_{20}$  in detail), and then we perform by-eye examinations of each object to keep only those candidates that show apparent interaction signatures (eg., tidal tails, distorted morphology, and double nuclei). This results in a sample of 56 merging systems.

For a fair comparison with isolated galaxies we also construct a sample of 1800 **control pairs**, each of which consists of two galaxies randomly selected from galaxies that are isolated, with no spectroscopic companion within  $100 h^{-1}\text{kpc}$  or photometric companion (with observed  $\Delta m_R < 1$  mag) within  $30 h^{-1}\text{kpc}$ . Isolated galaxies have the same magnitude and color cut as adopted for interacting galaxies.

### 2.3. Stellar Mass and Total IR Luminosity

Stellar masses are derived from rest-frame  $(B - V)$  colors and absolute  $M_B$  magnitude as described by the models of Bell & de Jong (2001) and Bell et al. (2005), who find a scatter of  $\sim 0.3$  dex in the resulting stellar mass estimates. These measurements were further refined by comparison with the stellar masses derived by Bundy et al. (2006) using detailed fits to the spectral energy distribution (SED). Empirically we find that the difference between the masses estimated using the rest-frame colors and the SED fits is improved by making small corrections for the redshift, rest-frame  $(U - B)$  and  $(B - V)$  colors:

$$\log_{10} \frac{M_*}{M_\odot} = -0.4(M_B - 5.48) + 1.737(B - V) + 0.098(U - B) - 0.130(U - B)^2 - 0.268z - 1.003. \quad (1)$$

These terms have the effect of correcting the  $z = 0$  measurements of Bell & de Jong (2001) to the galaxy redshift as well as accounting for evolution in color. Masses estimated from Equation 1 agree with those from full SED fits (when available; Bundy et al. 2006) to an rms accuracy of 0.25 dex.

Local studies have shown that the rest-frame MIR luminosity is tightly correlated with the total IR luminosity over a wide range of galaxy types (Roussel et al. 2001; Papovich & Bell 2002). This relation appears to hold up reasonably well to  $z \sim 1$  (Elbaz et al. 2002; Appleton et al. 2004) and hence allows us to estimate the IR luminosity from the observed flux of  $24 \mu\text{m}$  corresponding to the rest-frame  $11\text{-}21 \mu\text{m}$  flux over the redshift range  $0.1 < z < 1.1$ . Following the same procedure adopted by Le Floc’h et al. (2005), we convert the observed  $24 \mu\text{m}$  flux into the total IR luminosity by fitting for each source using SEDs from Chary & Elbaz (2001).<sup>1</sup> Because of the large PSF (FWHM  $6''$ ) of the  $24 \mu\text{m}$  data, we work on the total IR luminosity in pairs rather than the IR luminosity of each individual galaxy. This also allows us to make comparisons to local ULIRGs, which are found to be highly distorted merging systems (Sanders 1988; Borne et al. 1999), and to merger simulations in the literature (Barnes 2004; Jonsson et al. 2006), which yield the total star formation rate of the merger system. For each pair, we then calculate the mean IR luminosity-to-mass ratio,  $L_{IR}/M_*$ , by summing the IR luminosity of both galaxies and dividing by the total stellar mass of both components.

---

<sup>1</sup>Various template libraries lead to a scatter in this conversion of a factor of 2-3 (Le Floc’h et al. 2005).

### 3. RESULTS

Figure 1 shows the relation between  $L_{IR}$  and  $M_*$  for three of the galaxy samples. A relatively tight correlation is seen for the control pairs, and the close pairs and mergers are within the bounds of this relation but tend to occupy the upper region of  $L_{IR}$  for a given  $M_*$ . In the highest redshift bin, the fraction of merging galaxies and close pairs more massive than  $2 \times 10^{10} M_\odot$  that are ULIRGs is  $7.1\% \pm 4.3\%$ , compared to  $2.6\% \pm 0.7\%$  for the control sample. To address quantitatively the difference of  $L_{IR}$  among those samples, we compute the median  $L_{IR}/M_*$  for each sample. Using the median value of  $L_{IR}/M_*$  rather than performing the K-S test avoids the problem of handling the upper limits. When calculating the median  $L_{IR}/M_*$ , stellar mass cuts are further applied in each redshift bin (see Table 1). Over the entire redshift range, the median  $L_{IR}/M_*$  of pairs and mergers is twice ( $1.9 \pm 0.4$ ) that of the control sample. To assess if our results are sensitive to the method we have adopted to estimate stellar masses, we also apply the same analysis on a subsample of the data with stellar mass measurements derived from the SED-fitting procedure of Bundy et al. (2006). The enhancement in  $L_{IR}/M_*$  increases to  $3.1 \pm 1.3$  in this case, consistent with our initial result within the  $1\sigma$  uncertainties.

An alternative way to investigate the effect of galaxy interactions on the star formation rate is to study the dependence of  $L_{IR}/M_*$  on the pair separation, as shown in Figure 2. For comparison, distributions of  $L_{IR}/M_*$  in control pairs are also shown along the right-hand axes. The merging galaxies and close pairs possess higher median  $L_{IR}/M_*$  than wide pairs and control pairs, as shown in Table 1, but also have a wider spread in  $L_{IR}/M_*$ . The declining envelope of  $L_{IR}/M_*$  as a function of  $\Delta r_p$  is similar to the behavior of the local pair results reported by Barton et al. (2000), who use various sets of emission lines as the star formation tracer. The median  $L_{IR}/M_*$  of wide pairs, on the other hand, becomes close to that of the control pairs, indicating that the effect of galaxy interaction on star formation activity is limited to several tens of  $h^{-1}\text{kpc}$ .

### 4. DISCUSSION AND CONCLUSION

Using data from the DEEP2 Galaxy Redshift Survey with MIPS  $24 \mu\text{m}$  imaging in the EGS, we find that the combined IR luminosity at a given stellar mass of blue merging galaxies and kinematic close pairs is greater by a factor of  $1.9 \pm 0.4$  than that of control pairs randomly drawn from blue isolated galaxies. This enhancement is consistent with low-redshift studies of the SFR in galaxy pairs (Lambas et al. 2003; Nikolic, Cullen, & Alexander 2004). In addition, we also observe a declining envelope of the  $L_{IR}/M_*$  with increased projected separation of kinematic galaxy pairs. Based on the assumption that the IR emission is tightly

associated with the SFR, our results qualitatively support the picture of tidally triggered starbursts as predicted in hydrodynamic simulations, although the effect is apparently not large. The frequency of ULIRGs in massive interacting systems is only  $7.1\% \pm 4.3\%$  in the highest redshift bin ( $0.75 < z < 1.1$ ), and no ULIRGs are found below a combined stellar mass for the pair of  $4 \times 10^{10} M_{\odot}$ . The mass ratio between two gas-rich galaxies may be a key element in generating ULIRG luminosities (Dasyra et al. 2006), along with the dependence on the combined stellar mass of the interacting system. The wide spread of specific star formation rates in interacting galaxies found here (as inferred from the broad distribution of  $L_{IR}/M_*$ ), and also seen in Barton et al. (2000), indicates that some other mechanism(s) may determine the strength of the induced star formation as well – e.g., the galaxy structure, the mass/luminosity ratio, the orbital configuration, and the existence of AGN and/or bar. For example, studies by Lambas et al. (2003) and Woods, Geller, & Barton (2006) suggest that pairs with comparable luminosity do show stronger star formation activity than pairs with a larger luminosity contrast. The scatter in  $L_{IR}/M_*$  that we find could also be due to the fact that these systems are in different stages of merging: some kinematic pairs are likely on their first approach while others are being seen after their first passage. Another possibility is that some of the close pairs selected by our  $\Delta r_p$  and  $\Delta v$  criteria are not physical close pairs in real space (as opposed to redshift space; Perez et al. 2006). Our results nevertheless provide a constraint on the amount of induced star formation activity due to galaxy interactions at  $z \sim 0.1 - 1.1$ .

Finally, we note that tidally triggered star formation contributes moderately to the high IR luminosity density at intermediate redshifts of  $0.4 < z < 1.1$ . Lin et al. (2004) estimated that the pair fraction ( $\Delta r_p \leq 50 h^{-1} \text{kpc}$  and  $\Delta v \leq 500 \text{ km s}^{-1}$ ) of  $L^*$  galaxies over this redshift range is less than 15% and that the redshift evolution in the pair fraction is also much lower than the rapid decline of IR luminosity density seen with decreasing redshift. Additionally, the fraction of morphologically identified merging galaxies remains roughly constant at 7% up to  $z \sim 1$  (Lotz et al. 2006). These results, when combined with the moderate increase of star formation activity seen in interacting systems shown here, indicate that the contribution of galaxy interactions to the total IR density at intermediate redshift is  $\lesssim 36\%$ . This is consistent with the conclusions from the studies of IR populations of various morphology types by Bell et al. (2005) and Melbourne, Koo, & Le Floch (2005).

This Letter was prepared as part of the All-Wavelength Extended Groth International Survey (AEGIS) collaboration. We thank S. M. Faber and P. Jonsson for useful discussions and the anonymous referee for valuable comments; L. Lin acknowledges support from Taiwan COSPA project, and from Taiwan NSC grant NSC94-2112-M-002-026 and NSC93-2917-I-002-008. C. J. Conselice acknowledge an NSF Astronomy and Astrophysics Fellowship and

PPARC for support. A. L. Coil is supported by NASA through Hubble Fellowship grant HF-01182.01-A. The DEEP2 project was supported by NSF grants AST00-71198, AST05-07428 and AST05-07483. This work is based in part on observations made with the *Spitzer Space Telescope*, which is operated by the Jet Propulsion Laboratory, California Institute of Technology, under a contract with NASA. Support for this work was provided by NASA through contract 1255094 issued by JPL/Caltech. We close with thanks to the Hawaiian people for use of their sacred mountain.

## REFERENCES

- Appleton, P. N. et al. 2004, ApJS, 154, 147
- Barnes, J. E. 2004, MNRAS, 350, 798
- Barton, E. J., Geller M. J., & Kenyon S. J. 2000, ApJ, 530, 660
- Bell, E. F. & de Jong, R. S. 2001, ApJ, 550, 212
- Bell, E. F. et al. 2005, ApJ, 625, 23
- Bergvall, N., Laurikainen, E., & Aalto, S. 2003, A&A, 405, 31
- Borne, K. D., et al. 1999, Ap&SS, 266, 137
- Bundy, K., Fukugita, M., Ellis, R. S., Kodama, T., & Conselice, C. J. 2004, ApJ, 601, L123
- Bundy, K., et al. 2006, ApJ, 651, 120
- Carlberg, R. G., et al. 2000, ApJ, 532, L1
- Chary, R. & Elbaz, D. 2001, ApJ, 556, 562
- Coil, A. L., et al. 2004, ApJ, 609, 525
- Conselice, C. J. 2003, ApJS, 147, 1
- Conselice, C. J., Bershad, M. A., Dickinson, M., & Papovich, C. 2003, AJ, 126, 1183
- Cox, T. J. 2004, PhD thesis, UC Santa Cruz
- Dasyra et al. 2006, ApJ, 638, 745
- Davis, M., et al. 2003, SPIE, 4834, 161 (astro-ph/0209419)

- Davis, M., et al. 2007, this volume
- Elbaz, D., Cesarsky, C. J., Chanical, P., Aussel, H., Franceschini, A., Fadda, D., & Chary, R. R. 2002, *A&A*, 384, 848
- Jonsson, P., Cox, T. J., Primack, J. R., & Somerville, R. S. 2006, *ApJ*, 637, 255
- Lambas, D. G., Tissera, P. B., Alonso, M. S., & Coldwell, G. 2003, *MNRAS*, 346, 1189
- Larson, R. B., & Tinsley, B. M. 1978, *ApJ*, 219, 46
- Le Floch, E., et al. 2005, *ApJ*, 632, 169
- Lin, L. et al. 2004, *ApJ*, 617, L9
- Lotz, J. M., Primack, J., & Madau, P. 2004, *AJ*, 128, 163
- Lotz, J. M., et al. 2007, *ApJ* submitted (astro-ph/0602088)
- Melbourne, J., Koo, D. C., & Le Floch, E. 2005, *ApJ*, 632, L65
- Mihos, J. C., & Hernquist, L. 1996, *ApJ*, 464, 641
- Nikolic, B., Cullen, H., & Alexander, P. 2004, *MNRAS*, 355, 874
- Papovich, C., & Bell, E. F. 2002, *ApJ*, 579, L1
- Patton, D. R., et al. 2002, *ApJ*, 565, 208
- Perez, M. J., Tissera, P. B., Lambas, D. G., & Scannapieco, C. 2006, *A&A*, 449, 23
- Rieke, G. H., et al. 2004, *ApJS*, 154, 25
- Roussel, H., Sauvage, M., Vigroux, L., & Bosma, A. 2001, *A&A*, 372, 427
- Sanders, D. B., et al. 1988, *ApJ*, 325, 74
- Weiner, B. J., et al. 2005, *ApJ*, 620, 595
- Willmer, C. N. A., et al. 2006, *ApJ*, 647, 853
- Woods, D. F., Gellar, M. J., & Barton, E. J. 2006, *AJ*, 132, 197

Table 1. Properties of the pair sample

$z$	Sample	$M_B$ (individual)	$M_*$ (combined)	$No.$	$d_{24}$	median $L_{IR}/M_*$
0.1 < $z$ < 0.4	MG	$-21.7 \leq M_B \leq -18.7$	$9.7 \leq \log_{10} M_* \leq 10.7$	3(9)	...	...
...	close pair	$-21 \leq M_B \leq -18$	$9.7 \leq \log_{10} M_* \leq 10.7$	10(10)	68±10(%)	2.2±0.7
...	wide pair	$-21 \leq M_B \leq -18$	$9.7 \leq \log_{10} M_* \leq 10.7$	17(20)	89±6(%)	1.3±0.1
...	control pair	$-21 \leq M_B \leq -18$	$9.7 \leq \log_{10} M_* \leq 10.7$	480(600)	74±11(%)	1.0±0.3
0.4 < $z$ < 0.75	MG	$-22.7 \leq M_B \leq -19.7$	$10 \leq \log_{10} M_* \leq 11$	13(18)	62±13(%)	3.1±0.8
...	close pair	$-22 \leq M_B \leq -19$	$10 \leq \log_{10} M_* \leq 11$	21(24)	71±7(%)	2.7±0.4
...	wide pair	$-22 \leq M_B \leq -19$	$10 \leq \log_{10} M_* \leq 11$	44(54)	64±5(%)	1.7±0.3
...	control pair	$-22 \leq M_B \leq -19$	$10 \leq \log_{10} M_* \leq 11$	502(600)	60±7(%)	1.5±0.4
0.75 < $z$ < 1.1	MG	$-23.7 \leq M_B \leq -20.7$	$10.3 \leq \log_{10} M_* \leq 11.3$	20(29)	73±10(%)	3.3±2.7
...	close pair	$-23 \leq M_B \leq -20$	$10.3 \leq \log_{10} M_* \leq 11.3$	22(22)	76±7(%)	3.8±0.8
...	wide pair	$-23 \leq M_B \leq -20$	$10.3 \leq \log_{10} M_* \leq 11.3$	45(52)	62±5(%)	1.5±0.2
...	control pair	$-23 \leq M_B \leq -20$	$10.3 \leq \log_{10} M_* \leq 11.3$	547(600)	64±7(%)	1.9±0.5

Note. —  $M_B$  is the rest-frame  $B$ -band magnitude of each galaxy in pairs. The luminosity range of merging galaxies (MGs) is chosen to be twice as bright as that of individual galaxy in pairs because merging galaxies are assumed to be comprised of two galaxies.  $M_*$  is the stellar mass cut when computing the median  $L_{IR}/M_*$  and 24  $\mu\text{m}$  detection rate  $d_{24}$ . In the fifth column, the values outside (inside) the parentheses are the numbers of paired systems with (without) a stellar mass cut. Error bars quoted here are computed by bootstrapping.

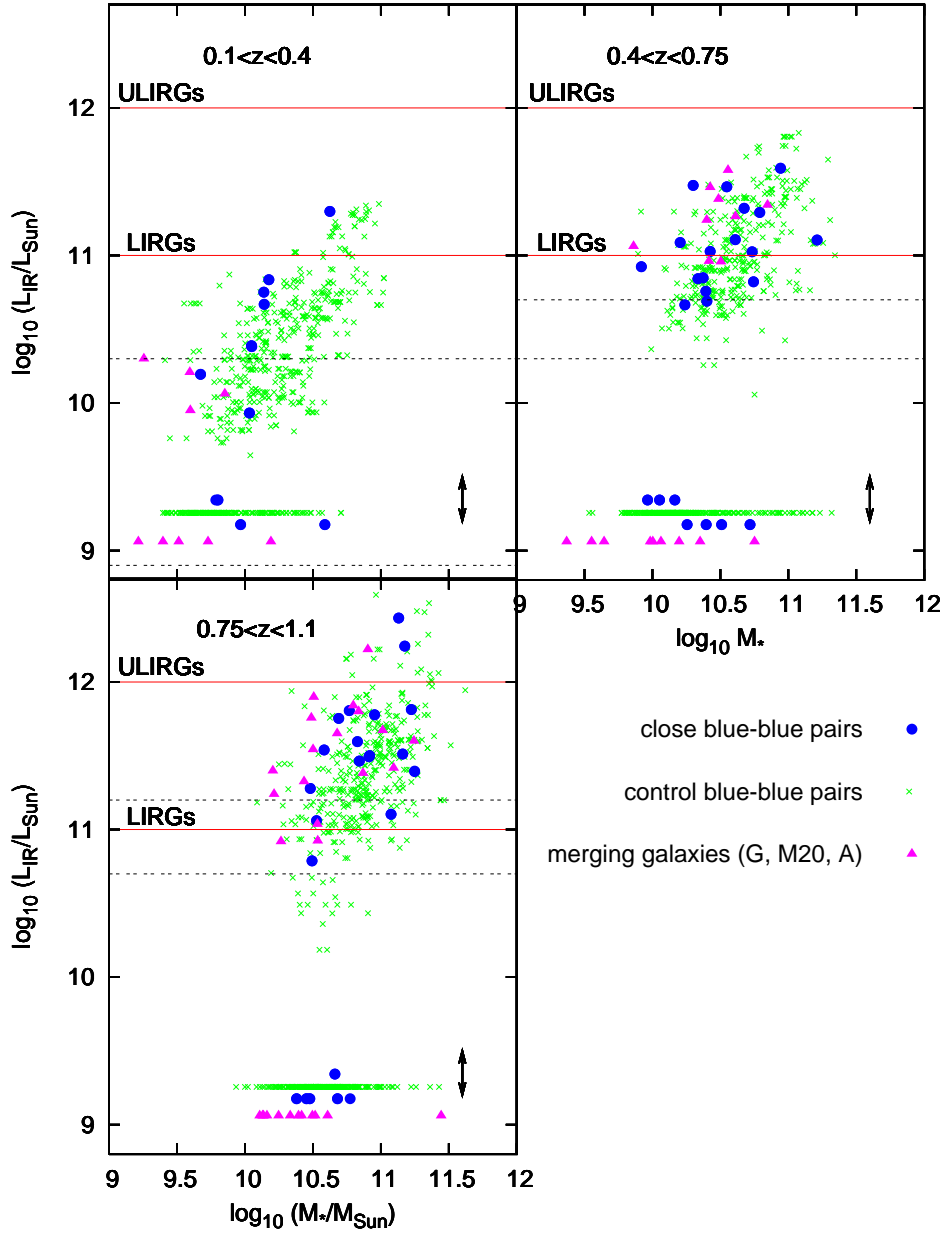


Fig. 1.— Total IR luminosity ( $L_{IR}$ ) vs. stellar mass ( $M_*$ ) for kinematic close pairs (blue circles), control pairs (green crosses), and morphologically identified merging galaxies (magenta triangles). Systems without a  $24 \mu\text{m}$  detection are assigned low  $L_{IR}$  values  $< 3 \times 10^9 L_{\odot}$ . Horizontal red solid lines represent the IR thresholds for ULIRGs ( $L_{IR} \geq 10^{12} L_{\odot}$ ) and LIRGs ( $L_{IR} \geq 10^{11} L_{\odot}$ ). Black dotted lines correspond to  $70 \mu\text{Jy}$  ( $5\sigma$ ) in  $24 \mu\text{m}$  at lower and upper redshift limits. Arrows in the lower right corner of each panel show the scatter (0.3 dex) in the conversion of  $24 \mu\text{m}$  flux into total  $L_{IR}$  between different template libraries. It can be seen that the close pairs and merging galaxies possess higher  $L_{IR}$  than control pairs for a given  $M_*$ .

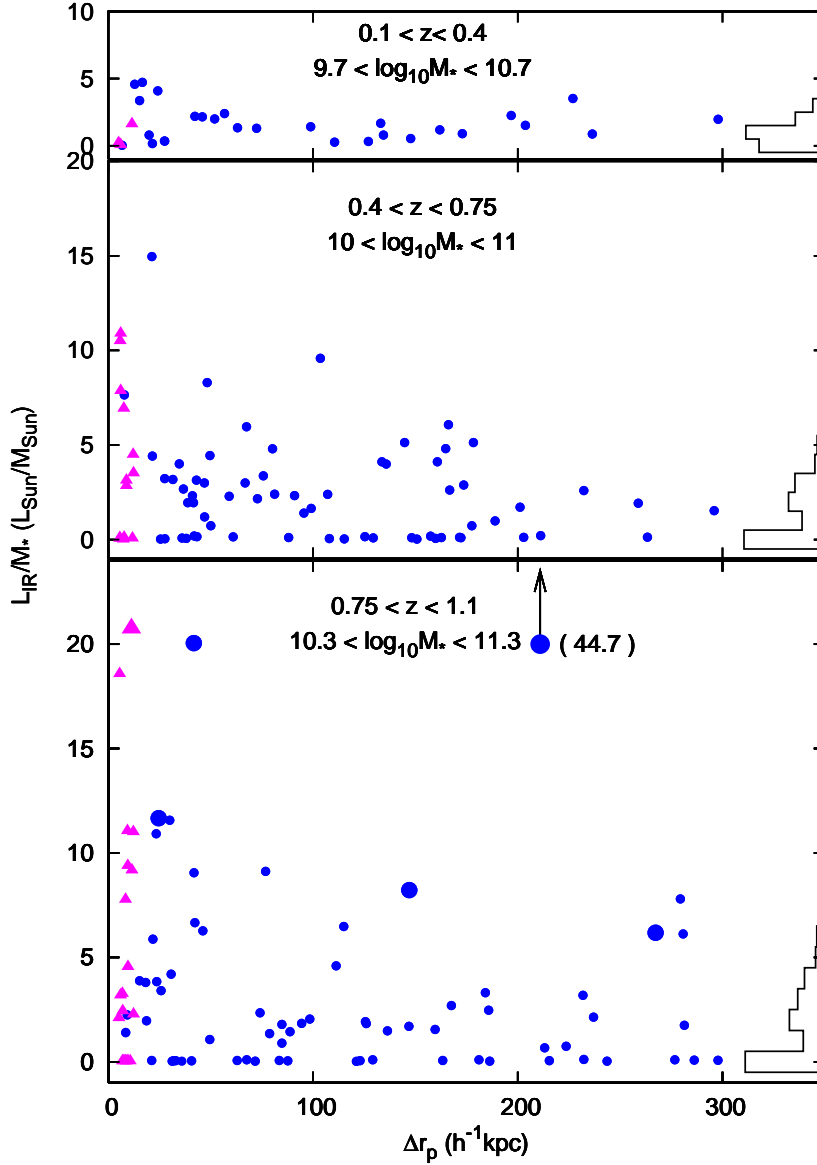


Fig. 2.—  $L_{IR}/M_*$  as a function of projected separation for kinematic galaxy pairs (blue circles) and merging galaxies (magenta triangles) in three redshift bins. Merging galaxies are assigned to  $\Delta r_p \sim 5 h^{-1}\text{kpc}$ , which is the minimum separation of kinematic close pairs. Galaxies with  $L_{IR} > 10^{12} L_{\odot}$  (ULIRGs) are shown as larger symbols. Distributions of  $L_{IR}/M_*$  in control pairs are also shown along the right-hand axes for comparison. Data points at  $L_{IR}/M_* = 0$  refer to those sources with no  $24 \mu\text{m}$  detection. The number within the parentheses in the bottom panel denotes the  $L_{IR}/M_*$  of the closest data point. Close pairs ( $\Delta r_p < 50 h^{-1}\text{kpc}$ ) and merging galaxies are found to have a higher median  $L_{IR}/M_*$  and a wider spread of  $L_{IR}/M_*$  than those of wide pairs ( $\Delta r_p > 50 h^{-1}\text{kpc}$ ) or control pairs (see Table 1).